Temperature dependence of Eu 4*f* and Eu 5*d* magnetizations in the filled skutterudite $EuFe_4Sb_{12}$

V. V. Krishnamurthy
Neutron Scattering Sciences Division, Oak Ridge National Laboratory, Oak Ridge, Tennessee 37831-6393, USA

D. J. Keavney, D. Haskel, J. C. Lang, and G. Srajer
Advanced Photon Source, Argonne National Laboratory, Argonne, Illinois 60439, USA

B. C. Sales and D. G. Mandrus
Materials Science and Technology Division, Oak Ridge National Laboratory, Oak Ridge, Tennessee 37831-6056, USA

J. L. Robertson
Neutron Scattering Sciences Division, Oak Ridge National Laboratory, Oak Ridge, Tennessee 37831-6473, USA
(Received 25 December 2007; revised manuscript received 18 November 2008; published 21 January 2009)

The element-specific and shell-specific magnetism of Eu in the filled skutterudite ferrimagnet $Eu_{0.95}Fe_4Sb_{12}$ has been investigated using Eu $M_{4,5}$- and Eu $L_{2,3}$-edge x-ray magnetic circular dichroism (XMCD) spectroscopy as a function of temperature. Eu L_3-edge x-ray absorption spectroscopy shows that Eu is mostly in the divalent state. Eu M_5-edge x-ray absorption spectroscopy, measured by electron yield, shows nearly equal fractions of Eu^{2+} and Eu^{3+} states because it probes a significant portion of the surface volume which is dominated by the Eu^{3+} impurity state. Sum-rule analysis of the Eu $M_{4,5}$-edge XMCD spectrum measured at 4.9 K yielded the 4*f* spin moment of $(7.15 \pm 0.3)\mu_B$ per Eu^{2+} ion. By comparing the Eu $L_{2,3}$-edge XMCD spectrum in the ferrimagnetic state of $Eu_{0.95}Fe_4Sb_{12}$ to that of a divalent Eu reference compound, the clathrate $Eu_8Ga_{16}Ge_{30}$, we show that the 5*d* spin polarization of Eu in the skutterudite is strongly enhanced by the exchange coupling with the 3*d* band electrons of Fe, which were shown to have an ordered moment of $-0.21\mu_B$/Fe in our earlier Fe $L_{2,3}$ XMCD measurements. The temperature dependence of the magnetic order parameter, determined from the Eu L_3-edge XMCD intensity, yields a mean-field-like exponent (~0.52) in the skutterudite and a three-dimensional Heisenberg-type (~0.36) exponent in the clathrate.

DOI: 10.1103/PhysRevB.79.014426 PACS number(s): 71.27.+a, 61.05.cj, 75.30.Mb, 75.50.Bb

I. INTRODUCTION

Filled skutterudites RM_4X_{12} (R=rare earth; M=Fe, Ru, and Os; and X=Sb and P) have attracted considerable interest because they exhibit a variety of correlated electron phenomena associated with an electronic ground state such as superconductivity, ferromagnetic ordering, antiferromagnetic ordering, and heavy-fermion behavior at low temperatures.[1,2] The filled skutterudites also have potential, such as thermoelectric materials, due to their large thermopower and lower electrical resistivity.[3] These materials crystallize in the cubic structure (space group *Im*3) with 2 f.u./unit cell. The rare-earth atoms fill the voids in the skutterudite structure of M_4X_{12}. The rattling motion of rare-earth atoms in the oversized atomic cages is believed to reduce the thermal conductivity while not significantly altering the electrical conductivity. La Knight-shift measurements in filled skutterudites using ^{139}La nuclear magnetic resonance (NMR) show strong correlation between the *d* bands of transition metal and the rattling motion of rare-earth atoms through electron-phonon coupling.[4] ^{121}Sb nuclear inelastic-scattering measurements in $EuFe_4Sb_{12}$ show that the vibrational density of states of Sb is lowered upon the filling of the cages by the rare-earth atoms.[5] The cubic crystal electric field at the rare-earth site plays an important role in determining the electronic ground state and the low-temperature magnetic and transport properties of these compounds. Despite several experimental and theoretical efforts on filled skutterudites, the mechanism of magnetic ordering in these compounds is not well understood, and the nature of magnetic interaction between the rare-earth and transition-metal ions is not clear. Therefore, detailed studies of the element-specific contributions to the total magnetization in magnetically ordered skutterudites are critically important to understand the role played by rare-earth ions, transition-metal ions, and conduction electrons in magnetic and thermal properties.

The valence-band structures of the narrow band-gap semiconductor $CoSb_3$ and related filled skutterudites AFe_4Sb_{12} (A=alkali metal, alkaline metal, or rare earth) consist of a manifold of Sb *p*-Fe 3*d*-derived states, with the *d* character concentrated just below the band edge, resulting in 24 valence electrons (n_v) per $FeSb_3$ unit, which include Sb *s* states.[6–8] While $CoSb_3$ (n_v=24) is nonmagnetic,[9] one may expect the *d*-derived density of states from the *M* atoms to increase as n_v is further reduced, leading to a Stoner instability toward magnetism. Ferromagnetic order would be anticipated because of the strongly hybridized electronic structure, which is, in fact, observed. While the nonsuperconducting metal $LaFe_4Sb_{12}$ (n_v=23.75) shows no magnetic ordering,[10] $CaFe_4Sb_{12}$, $SrFe_4Sb_{12}$, and $BaFe_4Sb_{12}$, with n_v=23.5, show nearly ferromagnetic metallic behavior,[11] and the n_v=23.25 compounds $NaFe_4Sb_{12}$ and KFe_4Sb_{12} are half-metallic ferromagnets.[12] The n_v=23.5 compounds, i.e., skutterudites that are filled with a divalent ion, are interesting because of their borderline ferromagnetic behavior.

The electronic properties of Eu-filled skutterudites are of particular interest because the variation in the Eu valency

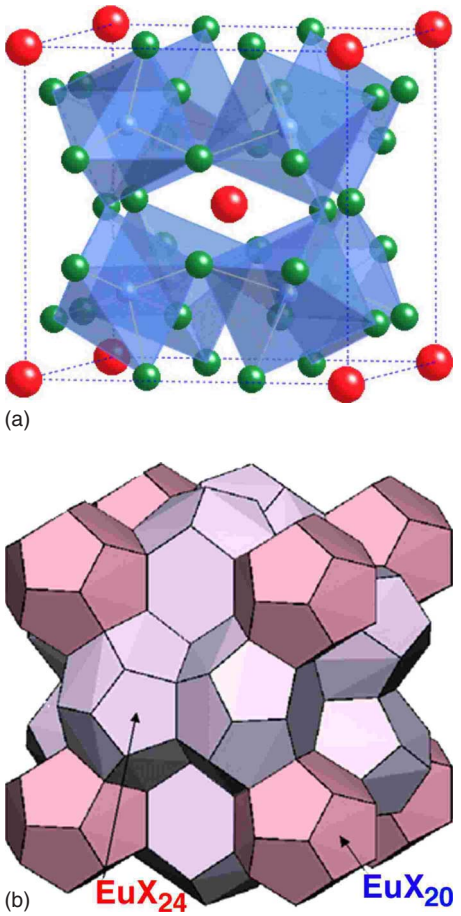

FIG. 1. (Color online) Crystal structures of the skutterudite and the clathrate. (a) Unit cell of the skutterudite $Eu_{0.95}Fe_4Sb_{12}$. Eu (large spheres) is at the corners and at the body center, Fe (smallest spheres) is located in the center of each octahedron (shown as semitransparent substructures), and Sb (medium sized spheres) is at the vertices of the octahedra. (b) The coordination polyhedra around Eu (not shown in figure) in the clathrate $Eu_8Ga_{16}Ge_{30}$. A Ga or Ge atom (X) is at each vertex of a polyhedron.

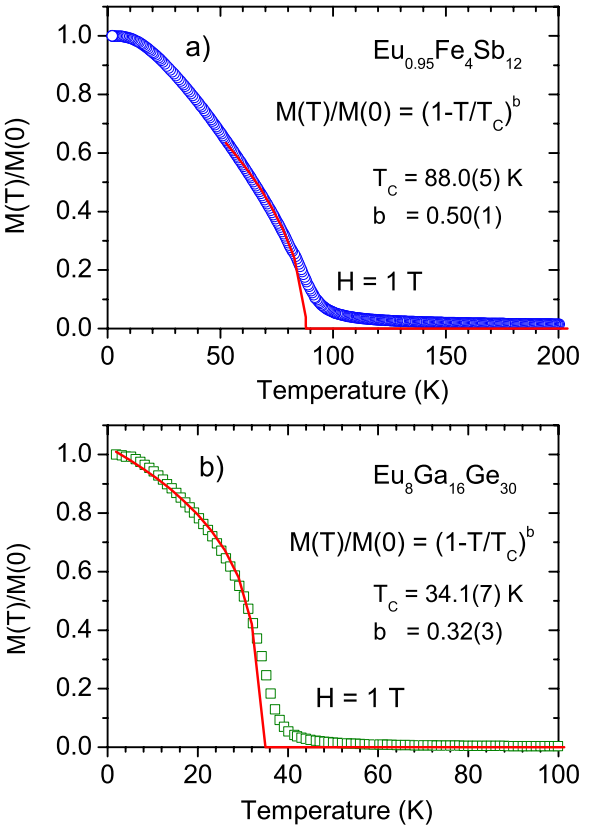

FIG. 2. (Color online) Temperature dependence of reduced magnetization, $M(T)/M(0)$, in (a) $Eu_{0.95}Fe_4Sb_{12}$ and (b) $Eu_8Ga_{16}Ge_{30}$, measured in a field of 1 T. The solid lines are best fits by the power law given in the figure (see text for the details of the fitting regions).

dramatically changes their magnetic properties. The Eu ion can be in a nonmagnetic trivalent state, a magnetic divalent state with a large free-ion-like moment ($7\mu_B$), or in a mixed-valence state with an average moment between 0 and $7\mu_B$. A mixed-valence state for Eu is another way to modify the band filling or n_v and hence alter the magnetic properties of the skutterudite. Similarly, the Eu site occupancy is also very important because it can modify the magnetic properties, such as the total magnetic moment, the transition temperature, Eu $4f$-Eu $4f$ interatomic interaction, and Eu $4f$-Fe $3d$ interatomic interaction.

Figure 1(a) shows the crystal structure of the Eu-filled skutterudite $Eu_{0.95}Fe_4Sb_{12}$. It is nearly metallic and orders ferrimagnetically with a Curie temperature of 85 K.[13,14] dc magnetization measurements on our polycrystalline specimens, presented in Fig. 2, show that the net magnetic moment of the compound is about $5.1\mu_B$/f.u. at 5 K, similar to that found in single crystals.[14,15] Eu L_3-edge x-ray absorption spectroscopy[16,17] measurements by Bauer *et al.*[14] in EuT_4Sb_{12} (T=Fe, Ru, Os) indicated nearly divalent Eu configuration without any change in the Eu^{2+} population with temperature. ^{151}Eu Mössbauer spectroscopy measurements and Eu L_3-edge x-ray absorption measurements by Grytsiv *et al.*[18] also indicated that Eu is nearly divalent in $Eu_{0.83}Fe_4Sb_{12}$. ^{57}Fe Mössbauer spectroscopy measurements by Reissner *et al.*[19] showed that Fe has two different environments in $Eu_{0.88}Fe_4Sb_{12}$. The value of the magnetic moment in $Eu_{0.95}Fe_4Sb_{12}$ is only 73% of the value of a fully saturated Eu^{2+} ion (seven electrons in the $4f$ shell, L=0, S=7/2, and total magnetic moment $\mu=7\mu_B$). Using Eu $M_{4,5}$-edge and Fe $L_{2,3}$ x-ray magnetic circular dichroism (XMCD) spectroscopy, Eu L_3-edge x-ray absorption spectroscopy, and local spin-density calculations, we have recently demonstrated that the lower value of the magnetic moment per f.u. in $Eu_{0.95}Fe_4Sb_{12}$ originates from a combination of a small fraction of Eu ions having a nominal 3+ valence and the ferrimagnetic alignment of a $7\mu_B$ moment per Eu^{2+} site and a $-0.21\mu_B$ moment per Fe site.[20]

Polarization-dependent x-ray absorption is a powerful tool for element-specific magnetization measurements in transition metal and rare earth containing ferromagnets.[21–25] XMCD measurements can give an insight into the temperature and magnetic field dependence of element- and shell-specific magnetic moments. In this paper, we report the temperature dependence of the $4f$ and $5d$ electron magnetizations of Eu from Eu $M_{4,5}$-edge XMCD and Eu $L_{2,3}$-edge XMCD spectroscopies. The $M_{4,5}$-edge XMCD is associated

with the excitation of electrons from the 3*d* shell to 4*f* states of Eu; therefore it directly probes the magnetization of Eu in the 4*f* shell. The $L_{2,3}$-edge x-ray absorption spectra (XAS) corresponds to the 2*p* to 5*d* transition in Eu, and hence XMCD at the $L_{2,3}$ absorption edges of Eu probes its 5*d* magnetization. An XMCD effect is expected at the $L_{2,3}$ edges of Eu if there is an ordered 5*d* moment due to the on-site 4*f*-5*d* exchange,[26] intrasite 5*d*-3*d* exchange between Eu and Fe, or both. For Eu, the 4*f*-5*d* exchange integral is calculated to be 8 mRy; therefore a strong interaction between 4*f* local moments and 5*d* band electrons is thus expected.[27] Because Fe is magnetically ordered in $Eu_{0.95}Fe_4Sb_{12}$, as in AFe_4Sb_{12} (*A* =Na or K), it would be desirable to know if the 5*d* band of Eu is magnetically polarized through an interaction with Fe 3*d* band electrons, similar to the case of RFe_2 compounds.[26]

By comparing the $L_{2,3}$-edge XMCD measurement in $Eu_{0.95}Fe_4Sb_{12}$ with a suitable reference Eu compound, in which only the rare-earth ion is the magnetic ion and whose 4*f* magnetic moment is known from other measurements such as magnetization or neutron diffraction, the $L_{2,3}$-edge XAS and XMCD can give a good comparison of the 5*d* magnetic moments in the two compounds. Such a comparison can also help us understand the possible interaction between Eu 5*d* electrons and Fe 3*d* band electrons in $Eu_{0.95}Fe_4Sb_{12}$. For this purpose, we have measured the Eu $L_{2,3}$-edge XMCD in $Eu_8Ga_{16}Ge_{30}$, which works as a reference compound with a pure Eu^{2+} valence state and without a magnetic transition-metal ion. $Eu_8Ga_{16}Ge_{30}$ orders in the clathrate structure, which is described by the stacking combinations of EuX_{20} and EuX_{24} (*X*=Ga or Ge) polyhedra and is shown in Fig. 1(b). $Eu_8Ga_{16}Ge_{30}$ orders ferromagnetically below 34 ± 2 K, and the saturation magnetic moment of Eu is known to be $\sim 7\mu_B$.[28–32]

II. EXPERIMENTAL SECTION

Polycrystalline samples of $Eu_yFe_4Sb_{12}$ (*y* is less than or equal to 1) and $Eu_8Ga_{16}Ge_{30}$ were prepared from the purest available elements as described in detail previously in Refs. 19 and 20. Briefly, $Eu_yFe_4Sb_{12}$ was prepared directly from the elements in a carbon-coated, evacuated, and sealed silica tube. The tube was heated to 1030 °C for 40h, quenched into water bath, and then heated at 700 °C for 1 week to form the correct skutterudite phase. The clathrate compound $Eu_8Ga_{16}Ge_{30}$ could be prepared by several methods; the simplest of which was the direct arc melting of the constituent elements on a water-cooled copper hearth in an Ar atmosphere. Powder x-ray diffraction patterns measured at room temperature confirmed the formation of the desired compounds with no other phases present. The Eu site filling fraction *y* was estimated to be close to 0.95 from the intensity analysis of the x-ray diffraction patterns. The samples were further characterized by dc magnetization, which confirmed the ferromagnetic transition (see Fig. 2) in both samples. The magnetization, $M(T)$, was scaled by its lowest-temperature value, which is approximated as $M(0)$, and the reduced magnetization $M(T)/M(0)$ is displayed in Fig. 2 for both the skutterudite and the clathrate. The reduced magnetization could be fitted by the power law

$$M(T)/M(0) = (1 - T/T_C)^b, \quad (1)$$

where T_C is the transition temperature and *b* is an exponent. For the clathrate, we find a very good fit using the above equation for the entire temperature range. For the skutterudite, the best fit by the power law could be obtained for the $T \geq 50$ K region. The magnetization at low temperatures is likely to have more complex temperature dependence because there are two magnetic sublattices, one of Eu and the other of Fe, in this compound. The value of the T_C obtained from the fits agrees with the literature values for the respective compounds.[13,14,30,32] The exponent *b* values are given in Fig. 2.

The powder samples were ground, filtered through a 20 μm mesh, and coated onto tapes for Eu *L*-edge measurements. A multilayered tape, optimized for the L_3 absorption edge jump of Eu, was used in the XMCD measurements performed in the transmission geometry. XMCD at the Eu $L_{2,3}$ edges was measured at the hard x-ray beamline 4-ID-D at the Advanced Photon Source (APS) at Argonne National Laboratory. The helicity of the photons was modulated between left-circular polarization and right-circular polarization using a diamond (111) phase retarder operated near a Bragg angle in transmission geometry within the energy region of 6.9–7.7 keV. The XMCD spectra were measured in the lock-in detection mode[33] in the temperature range of 4.8–155 K in a 0.5 T horizontal field superconducting magnet. XMCD is defined as $\Delta\mu(E)=(\mu^+-\mu^-)$ and the x-ray absorption coefficient is defined as $\mu(E)=\frac{(\mu^+ + \mu^-)}{2}$, where μ^+ and μ^- are the x-ray absorption measured with positive and negative photon helicities, respectively. At each temperature, the XMCD spectrum was measured for parallel and antiparallel directions of the magnetic field relative to the photon wave vector and the resulting spectra were averaged. The value of the magnetic field used in the $L_{2,3}$-edge XMCD measurements varied in the range of 0.29–0.5 T. The XAS and XMCD at Eu $M_{4,5}$ and Fe $L_{2,3}$ edges in the skutterudite $Eu_{0.95}Fe_4Sb_{12}$ were measured at the soft x-ray beamline 4-ID-C at the APS. The measurements were performed by detecting the total electron yield on a hot pressed and highly polished pellet of polycrystalline sample at 2.3 K in an applied field of 2 T.

III. RESULTS AND DISCUSSION

A. XAS in $Eu_{0.95}Fe_4Sb_{12}$ and $Eu_8Ga_{16}Ge_{30}$

Figure 3 shows the XAS measured at Eu $L_{2,3}$ edges in $Eu_{0.95}Fe_4Sb_{12}$ and in the reference compound $Eu_8Ga_{16}Ge_{30}$. These spectra are normalized such that their L_3-edge jump is unity. The Eu $L_{2,3}$ XAS in $Eu_8Ga_{16}Ge_{30}$ has a single peak, and the edge energy determined from the derivative maximum comes out to be 6971 ± 0.5 eV, suggesting a pure Eu^{2+} valence state. In contrast, a strong peak and a satellite are observed in the Eu $L_{2,3}$ XAS spectra of $Eu_{0.95}Fe_4Sb_{12}$. The main peak is located exactly at the same energy as in $Eu_8Ga_{16}Ge_{30}$, confirming a dominant contribution from Eu^{2+} valence state. There is a satellite peak in the absorption spectra about 8 eV above the main position of the peak. Based on the position of this satellite with respect to the position of the

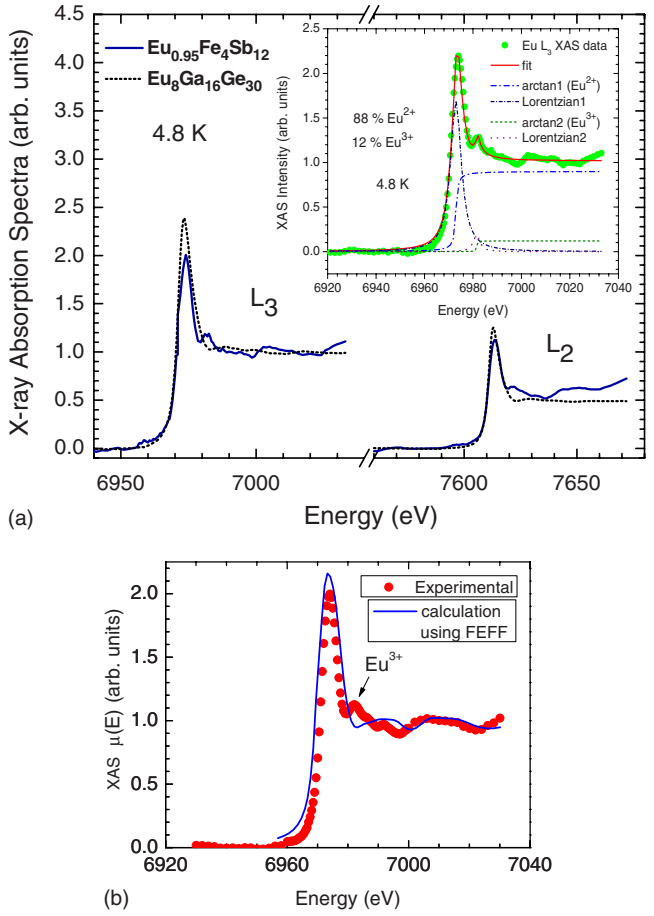

FIG. 3. (Color online) (a) Normalized x-ray absorption spectra at Eu L_3 and L_2 edges in $Eu_{0.95}Fe_4Sb_{12}$ and $Eu_8Ga_{16}Ge_{30}$ at 4.8 K in an applied field of 0.5 T. Inset shows the XAS with a fit to two-component arctangent step function with Lorentzian. (b) Experimental (filled circles) and FEFF calculation (solid line) of Eu L_3-edge x-ray absorption spectrum in $Eu_{0.95}Fe_4Sb_{12}$.

main peak, we identify the satellite with the Eu^{3+} valence state, which is in agreement with the $L_{2,3}$ absorption spectra reported for other mixed-valence Eu compounds, such as $EuNi_2Si_{2-x}Ge_x$.[34] To further establish the origin of this satellite peak, we have calculated the near-edge XAS at the L_3 edge of Eu in $EuFe_4Sb_{12}$ using FEFF8, an automated program for full multiple-scattering calculation with self-consistent potentials for the cluster of atoms.[35] The result, which is shown together with the experimental XAS in Fig. 3(b), shows that the satellite peak is not associated with the near-edge structure of Eu^{2+} ions in support of our interpretation. We have used arctangent as an *ad hoc* step function for representing the transition to the continuum states. The relative intensities of Eu^{2+} and Eu^{3+} ionic contributions are determined by fitting the XAS to a two-component model consisting of an arctangent step function and a Lorentzian peak for each valence state. Such a fit is often used for the analysis of mixed valence in rare-earth intermetallic compounds.[36] The fit was constrained such that the threshold energy for both the XAS (Lorentzian) peak and the step function for a given valence state is the same, i.e., same as in the model used by Godart *et al.*[36] for the analysis of Sm valence in $Sm_{1-x}Gd_xS$.

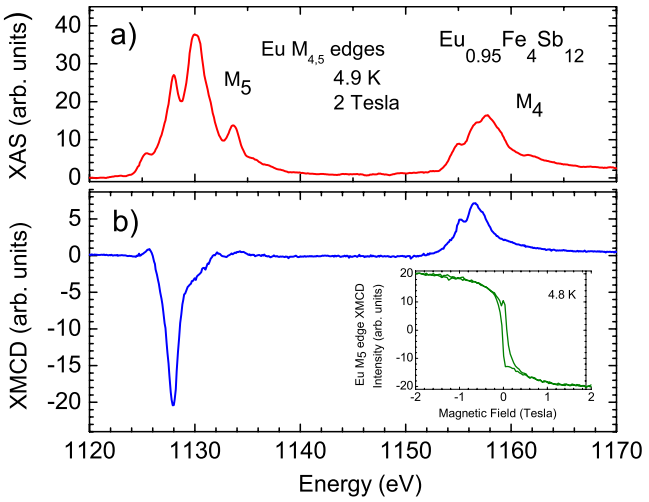

FIG. 4. (Color online) Eu $M_{4,5}$-edge (a) XAS and (b) XMCD in $Eu_{0.95}Fe_4Sb_{12}$ measured in a field of 2 T at 4.8 K. Inset shows the hysteresis of M_5-edge XMCD peak intensity at $E=1128.2$ eV measured at 4.8 K

This procedure yielded a valence state population of 88% for Eu^{2+} and 12% for Eu^{3+}. Inset of Fig. 3(a) shows Eu L_3-edge XAS, which is the fit that is shown by the solid line and the two components that are shown by different types of broken lines.

B. Eu $M_{4,5}$-edge XMCD in $Eu_{0.95}Fe_4Sb_{12}$

Figure 4 shows the XAS and XMCD at Eu $M_{4,5}$ edges in $Eu_{0.95}Fe_4Sb_{12}$ measured at 4.9 K in an applied field of 2 T. The XAS at the M_5 and M_4 edges show at least four peaks that can be associated with the multiplet splittings of Eu^{2+} and Eu^{3+} ions. The positions of these multiplet peaks are found to be nearly the same as the theoretical positions of Eu^{2+} and Eu^{3+} ions reported in the literature.[37,38] Then, the Eu M_4-edge XAS spectrum was fitted to linear combination of the theoretical XAS from Eu^{2+} and Eu^{3+}.[20] From the best fit, we find that the Eu^{2+} valence state has a $48\% \pm 2\%$ contribution and the Eu^{3+} valence state has a $52\% \pm 2\%$ contribution. We would like to note that the Eu^{3+} contribution estimated from the soft x-ray absorption measurement at the M_4 edge is much larger than the 12% found in the hard x-ray absorption spectroscopy measurement at the L_3 edge. We attribute the discrepancy to the higher fraction of the Eu^{3+} states, most likely from an impurity in the sample surface, which are preferentially probed in the soft x-ray absorption measurements (50 Å in total electron yield mode). The XMCD displayed in Fig. 4(b) has a negative sign for the M_5 edge and positive sign for the M_4 edge. Because the XMCD measured at the Eu $M_{4,5}$ edges is associated with a $3d$ initial state and a $4f$ final state, it directly gives a measure of the magnetic polarization in the $4f$ shell of Eu ions. The sum-rule analysis enables the estimation of spin and orbital magnetic moments of Eu from the measured intensities of XAS and XMCD spectra. For the $M_{4,5}$ edges of Eu, the sum rules[21] for the expectation values of the orbital angular momentum $\langle L_Z \rangle$ and the spin angular momentum $\langle S_Z \rangle$ can be written as

$$\langle L_Z \rangle = -\frac{(A_{M4} + A_{M5})N_{4f}}{\mu_0(M)} \quad (2)$$

and

$$\langle S_Z \rangle + (7/2)\langle T_Z \rangle = -\frac{(2A_{M5} - 3A_{M4})N_{4f}}{2\mu_0(M)}, \quad (3)$$

where $A_{M5}=\int_{M_5}\Delta\mu(E)dE$ is the integrated XMCD intensity at the Eu M_5 edge, $A_{M4}=\int_{M_4}\Delta\mu(E)dE$ is the integrated XMCD intensity at the Eu M_4 edge, N_{4f} is the number of holes in the 4f shell of Eu, $\mu_0(M)$ is the sum of the integrated XAS intensity at Eu M_5 and Eu M_4 edges, $\int_{M_5+M_4}\mu(E)dE$, and $\langle T_Z \rangle$ is the magnetic-dipole operator of Eu. $\mu_{\text{orb}}=-\langle L_Z \rangle$ and $\mu_{\text{tot}}=-(\langle L_Z \rangle+2\langle S_Z \rangle)$ are the orbital magnetic moment and the total magnetic moments of Eu, respectively. We assumed that $\langle T_Z \rangle=0$, as Eu site has a cubic symmetry in this compound. With the XAS and XMCD spectra, shown in Fig. 4, the Eu^{2+} valence population of $48\% \pm 2\%$ with the assumption of $N_{4f}=7$ yielded $\mu_{\text{orb}}=(0.13 \pm 0.1)\mu_B$ and $\mu_{\text{spin}}=(7.07 \pm 0.3)\mu_B$ per Eu^{2+} ion. The total moment per Eu^{2+} ion is therefore $(7.2 \pm 0.3)\mu_B$. The Eu 4f magnetic moment and the Fe 3d total magnetic moment, $\sim 0.21\mu_B$ per Fe, are almost antiferromagnetically coupled in $Eu_{0.95}Fe_4Sb_{12}$.[20]

Figure 5(a) shows the Eu M_5-edge XMCD at various temperatures both below and above the ferrimagnetic transition temperature of ~85 K. Figure 5(b) shows the temperature dependence of the integrated XMCD intensity of the individual peaks from Eu^{2+} and Eu^{3+} valence sites, extracted by fitting the data [shown in Fig. 5(a)] to three Lorentzian peaks. Note that the XMCD signal from Eu^{2+} state is strongly temperature dependent and clearly indicates the ferrimagnetic transition in the vicinity of 85 K. The XMCD signal from Eu^{3+} impurities shows a weak temperature dependence and does not indicate any magnetic transition.

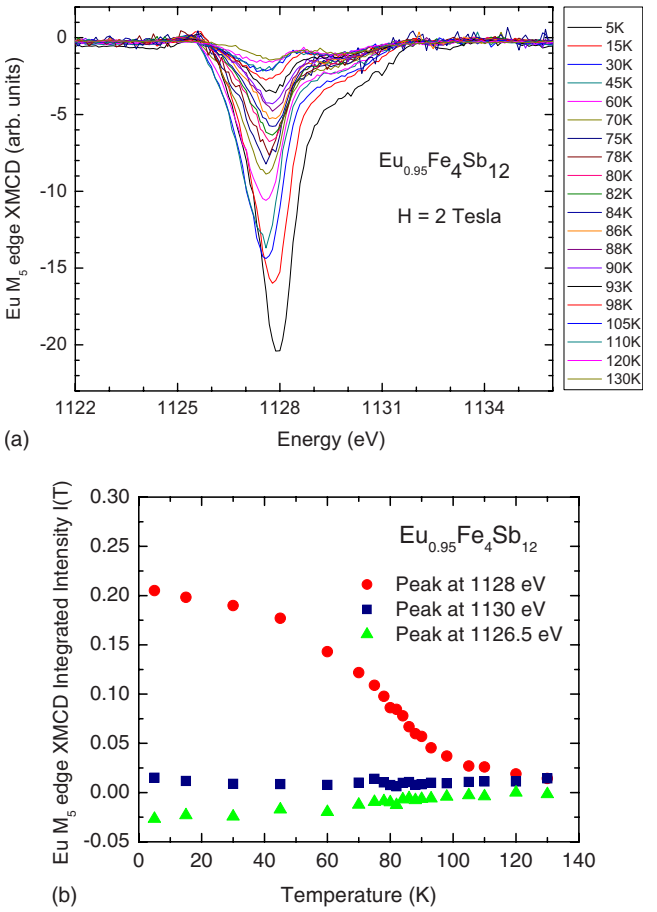

FIG. 5. (Color online) (a) Eu M_5-edge XMCD in $Eu_{0.95}Fe_4Sb_{12}$ measured in a field of 2 T in the temperature range of 5–130 K. (b) Temperature dependence of the integrated intensity from the 1128 eV (Eu^{2+}), 1130 eV (Eu^{3+}), and 1125.6 eV (Eu^{3+}) peaks in the Eu M_5-edge XMCD spectra in $Eu_{0.95}Fe_4Sb_{12}$.

C. Comparison of Eu $L_{2,3}$-edge XMCD in $Eu_{0.95}Fe_4Sb_{12}$ and $Eu_8Ga_{16}Ge_{30}$

XMCD spectra at the Eu $L_{2,3}$ edges in $Eu_{0.95}Fe_4Sb_{12}$ and $Eu_8Ga_{16}Ge_{30}$ measured on multilayered tape of samples at 4.8 K in an applied field of 0.5 T are presented in Figs. 6 and 7, respectively. Hysteresis measurements confirmed that the magnetization of Eu or the XMCD signal heights are saturated in a field of 0.5 T. The XMCD peak or minimum positions occur at the same edge energies in the two compounds and confirm that the magnetism originates from the Eu^{2+} ions in the two compounds. A comparison of the XMCD signal heights at the L_3 and L_2 edges in the two compounds indicate that the dichroism in the skutterudite is about a factor of 2 larger than the dichroism in the clathrate. The degree of polarization in the 5d shell or the 5d magnetic moment of Eu determines the intensity of the Eu $L_{2,3}$-edge XMCD signal in these compounds. Because the XMCD intensity is proportional to the magnetization or magnetic moment, the larger L-edge XMCD in the skutterudite implies that its Eu 5d moment is larger than the Eu 5d moment in the clathrate. Therefore, the Eu 5d moment in $Eu_{0.95}Fe_4Sb_{12}$ has

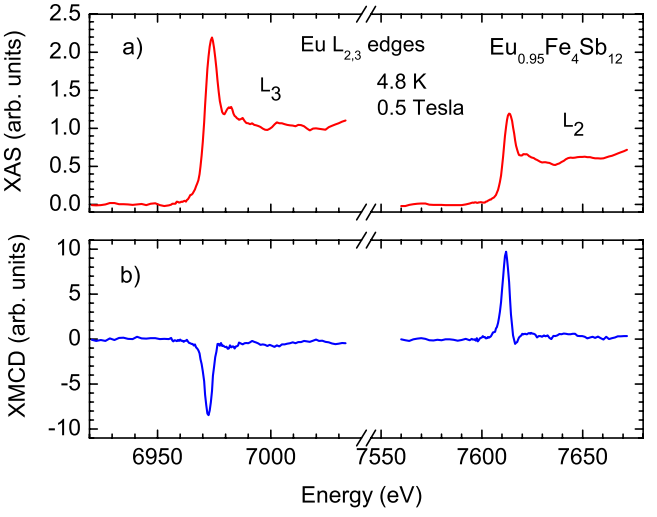

FIG. 6. (Color online) (a) XAS and (b) XMCD at the Eu $L_{2,3}$ edges in $Eu_{0.95}Fe_4Sb_{12}$ measured at 4.8 K in an applied field of 0.5 T.

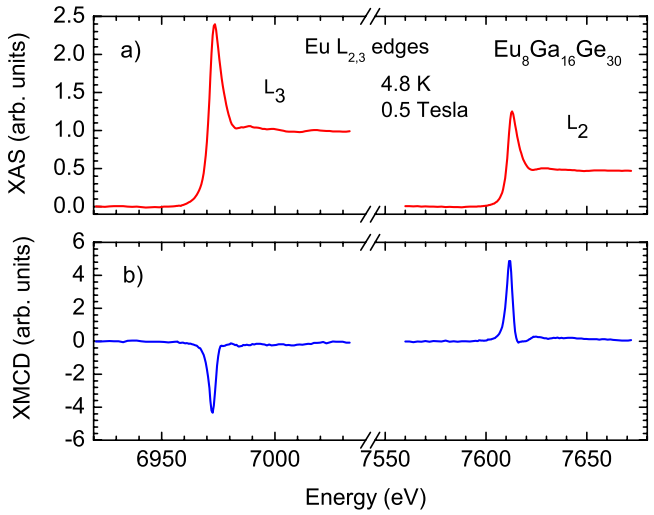

FIG. 7. (Color online) (a) XAS and (b) XMCD at the Eu $L_{2,3}$ edges in $Eu_8Ga_{16}Ge_{30}$ measured at 4.8 K in a field of 0.5 T.

significant contributions from both $4f$-$5d$ intra-atomic exchange interaction and $3d$-$5d$ interatomic exchange interaction with the $3d$ states of Fe.

D. Temperature dependence of Eu magnetization

Figure 8 shows the temperature dependence of the modulus of the Eu L_3-edge intensity, $I(T)$, measured at an energy of 6972.5 eV, where the XMCD amplitude is maximum in $Eu_{0.95}Fe_4Sb_{12}$ and $Eu_8Ga_{16}Ge_{30}$. Because $I(T)$ is directly proportional to the magnetization of Eu, M, its temperature dependence gives a direct measure of the order parameter at the

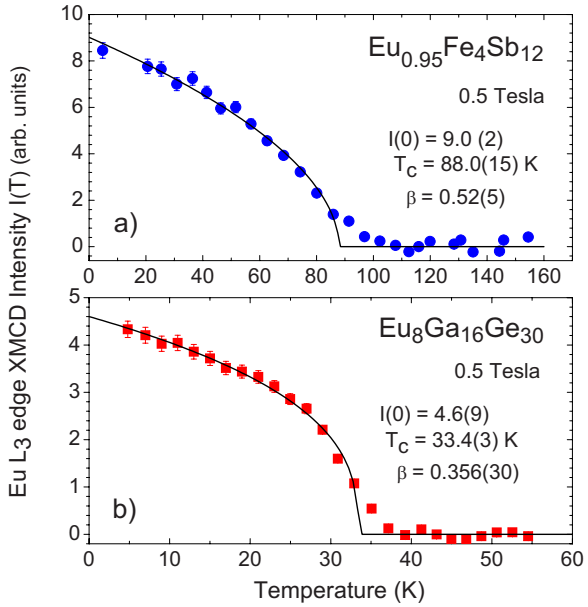

FIG. 8. (Color online) Temperature dependence of the Eu L_3-edge XMCD intensity, measured in a field of 0.5 T, shows the magnetic phase transitions in (a) $Eu_{0.95}Fe_4Sb_{12}$ and (b) $Eu_8Ga_{16}Ge_{30}$. The numbers in the brackets indicate the error in the last significant digits.

onset of long-range ferrimagnetic ordering ($Eu_{0.95}Fe_4Sb_{12}$) or ferromagnetic ordering ($Eu_8Ga_{16}Ge_{30}$) of Eu moments. The intensity $I(T)$, plotted in Fig. 8(a), is nearly zero for $T \gg 100$ K. It starts to increase as the sample is cooled below 100 K toward the ferrimagnetic ordering temperature of $Eu_{0.95}Fe_4Sb_{12}$. A similar behavior of the Eu L_3-edge XMCD intensity is also observed below 37 K in $Eu_8Ga_{16}Ge_{30}$, indicating a ferromagnetic ordering of the Eu moments. The temperature dependence of XMCD intensity $I(T)$ in the ferromagnetic state of the two compounds could be fit by the power law,

$$I(T) = I(0)(1 - T/T_C)^{\beta}, \tag{4}$$

where $I(0)$ is the intensity at $T=0$ K, T_C is the Curie temperature, and β is the magnetization exponent. The best fits are displayed as the solid lines over the data in Figs. 8(a) and 8(b). The fit presented in Fig. 8(a) yielded $I(0)=9.0\pm2$, $T_C=88\pm1.5$ K, and $\beta=0.52\pm0.05$ for $Eu_{0.95}Fe_4Sb_{12}$. The fitted value of T_C agrees with the values reported in the literature.[13,14] The value of β is in agreement with the mean-field theoretical prediction of the magnetization critical exponent 0.5.[39] The fit to the $I(T)$ in $Eu_8Ga_{16}Ge_{30}$ in Fig. 8(b) yielded $I(0)=4.6\pm0.09$, $T_C=33.4\pm0.3$ K, and $\beta=0.356\pm0.03$. The value of T_C returned by the fit is within the range of values, 32–36 K, reported in the literature.[30,32] The T_C and exponent β values found here for both the compounds also agree with the T_C and exponent b values found from the dc magnetization for the respective compounds in Sec. II. The value of the exponent β for $Eu_8Ga_{16}Ge_{30}$ agrees with the theoretical values of the magnetization critical exponents of three-dimensional (3D) models, $\beta=0.367\pm0.002$ of the 3D Heisenberg model[40] and $\beta=0.3485\pm0.0002$ of the 3D XY model.[41] The error bar on the theoretical exponent value accounts for the results from different theoretical approaches reported in the literature.[40,41] The applied field plays the role of aligning magnetic domains in the ferromagnetic or ferrimagnetic state, and it does not induce any additional moment. Therefore the measured XMCD signal gives a good measure of the order parameter in the magnetically ordered state. Above T_C, the large applied field can induce magnetization in the critical paramagnetic region and hence result in an XMCD signal, and the magnetic transition appears broadened. The bulk magnetization, shown in Fig. 2, also shows broadening of the transition in a field of 7 T. Therefore, the applied field induces additional error in the exponent values. The error bars reported above already include this contribution.

The ferrimagnetic ordering of Eu, as proven by the observation of the phase transition at $T_C=88\pm1.5$ K in the temperature dependence of Eu L_3-edge XMCD, suggests that Eu plays a dominant role in the onset of metallic ferrimagnetism. The evidence of bandlike $5d$ states of Eu and the metallic behavior in the resistivity are consistent with the ferrimagnetic ordering mediated by the coupling of Eu $4f$ moment with the nearly ferromagnetic conduction-electron band of the $[Fe_4Sb_{12}]^{2.2-}$ host lattice through Eu $5d$ states.[20] A similar coupling between Gd and Fe has been recently reported to account for the ferromagnetic ordering in $GdFe_2Zn_{20}$.[42] While Eu plays a key role in the magnetic

ordering in $Eu_{0.95}Fe_4Sb_{12}$, Yb has no detectable magnetic moment in the Zintl phase compound $Yb_{14}MnSb_{11}$, in which only Mn orders ferromagnetically below 53 K.[43] Yet these two compounds have interesting thermoelectric properties.[44,45] It would be interesting to compare and contrast the magnetic and thermoelectric properties of such compounds to know the role played by intra-atomic and interatomic exchange interactions in electrical conductivity and thermal transport properties. We suggest first-principles electronic structure calculations of magnetic properties, including the XMCD spectra at Eu M edges and Eu L edges in these compounds, for more insights into the relation between the magnetism and thermopower and electrical conductivity in this class of materials.

IV. SUMMARY

The valence of Eu and temperature dependence of the element-specific and shell-specific magnetic behavior of Eu in the filled skutterudite ferrimagnet $Eu_{0.95}Fe_4Sb_{12}$ have been investigated using x-ray absorption and x-ray magnetic circular dichroism spectroscopies at the Eu $M_{4,5}$ edges and at the Eu $L_{2,3}$ edges. Bulk sensitive Eu L_3 XAS indicates that Eu ions are in the divalent state in the pure skutterudite phase. The total magnetic moment of Eu is shown to be $(7.2 \pm 0.3)\mu_B$ per Eu^{2+} ion which is mostly antiparallel to magnetic moment on the Fe sites. Strong temperature dependence of the XMCD from Eu^{2+} ions has been observed in the measurements at the Eu $M_{4,5}$ edges. The Eu $L_{2,3}$ XAS/XMCD are compared with the divalent Eu ferromagnetic ($T_C = 34 \pm 2$ K) clathrate reference compound $Eu_8Ga_{16}Ge_{30}$. The Eu L_3-edge XMCD signal in the skutterudite is found to be nearly twice that of the clathrate, indicating a substantial enhancement of the Eu 5*d* polarization arising from the 5*d*-3*d* interatomic exchange interaction. The temperature dependence of the Eu L_3-edge XMCD gives a measure of the order parameter in the magnetically ordered state below T_C and confirms that there exists a strong on-site exchange coupling between localized 4*f* moment and the 5*d* conduction electrons of Eu in both $Eu_{0.95}Fe_4Sb_{12}$ and $Eu_8Ga_{16}Ge_{30}$.

ACKNOWLEDGMENTS

The authors would like to gratefully acknowledge very helpful discussion with D. J. Singh. This research is sponsored by Materials Science and Engineering Division, Scientific User Facilities Division, Office of Basic Energy Sciences, U.S. Department of Energy under Contract No. DE-AC05-00OR22725 with Oak Ridge National Laboratory, managed by UT-Battelle, LLC. The work at the APS, Argonne National Laboratory is sponsored by the Office of Sciences, U.S. Department of Energy under Contract No. DE-AC02-06CH11357.

[1] B. C. Sales, in *Hand Book on the Physics and Chemistry of Rare Earths*, edited by K. A. Gschneidner, Jr., J.-C. G. Buenzli, and V. K. Pecharsky (Elsevier, New York, 2003), Vol. 33, pp. 1–34.
[2] M. B. Maple, N. R. Dilley, D. A. Gajewski, E. D. Bauer, E. J. Freeman, R. Chau, D. Mandrus, and B. C. Sales, Physica B **259-261**, 8 (1999).
[3] V. Keppens, D. Mandrus, B. C. Sales, B. C. Chakoumakos, P. Dai, R. Coldea, M. B. Maple, D. A. Gajewski, E. J. Freeman, and S. Bennington, Nature (London) **395**, 876 (1998).
[4] Y. Nakai, K. Ishida, K. Magishi, H. Sugawara, D. Kikuchi, and H. Sato, J. Magn. Magn. Mater. **310**, 255 (2007).
[5] H. C. Wille, R. P. Hermann, I. Sergueev, O. Leupold, P. van der Linden, B. C. Sales, F. Grandjean, G. J. Long, R. Ruffer, and Y. V. Shvydko, Phys. Rev. B **76**, 140301(R) (2007).
[6] L. Nordstrom and D. J. Singh, Phys. Rev. B **53**, 1103 (1996).
[7] D. J. Singh and W. E. Pickett, Phys. Rev. B **50**, 11235 (1994).
[8] D. J. Singh and I. I. Mazin, Phys. Rev. B **56**, R1650 (1997).
[9] K. Koga, K. Akai, K. Oshiro, and M. Matsuura, Phys. Rev. B **71**, 155119 (2005).
[10] M. E. Danebrock, C. B. H. Evers, and W. Jeitschko, J. Phys. Chem. Solids **57**, 381 (1996).
[11] E. Matsuoka, K. Hayashi, A. Ikeda, K. Tanaka, T. Takabatake, and M. Matsumura, J. Phys. Soc. Jpn. **74**, 1382 (2005).
[12] A. Leithe-Jasper, W. Schnelle, H. Rosner, N. Senthilkumaran, A. Rabis, M. Baenitz, A. Gippius, E. Morozova, J. A. Mydosh, and Y. Grin, Phys. Rev. Lett. **91**, 037208 (2003); A. Leithe-Jasper, W. Schnelle, H. Rosner, M. Baenitz, A. Rabis, A. A. Gippius, E. N. Morozova, H. Borrmann, U. Burkhardt, R. Ramlau, U. Schwarz, J. A. Mydosh, Y. Grin, V. Ksenofontov, and S. Reiman, Phys. Rev. B **70**, 214418 (2004).
[13] E. Bauer, St. Berger, A. Galatanu, M. Galli, H. Michor, G. Hilscher, Ch. Paul, B. Ni, M. M. Abd-Elmeguid, V. H. Tran, A. Grytsiv, and P. Rogl, Phys. Rev. B **63**, 224414 (2001).
[14] E. D. Bauer, A. Slebarski, N. A. Frederick, W. M. Yuhasz, M. B. Maple, D. Cao, F. Bridges, G. Giester, and P. Rogl, J. Phys.: Condens. Matter **16**, 5095 (2004).
[15] Brian C. Sales, Rongying Jin, David Mandrus, and Peter Khalifah, Phys. Rev. B **73**, 224435 (2006).
[16] J. Roehler, in *Handbook on Physics and Chemistry of the Rare Earths*, edited by S. Huefner and L. Eyring (North-Holland, Amsterdam, 1987), Vol. 10, p. 453.
[17] G. Wortmann, Hyperfine Interact. **47–48**, 179 (1989).
[18] A. Grytsiv, P. Rogl, S. Berger, C. Paul, E. Bauer, C. Godart, B. Ni, M. M. Abd-Elmeguid, A. Saccone, R. Ferro, and D. Kaczorowski, Phys. Rev. B **66**, 094411 (2002).
[19] M. Reissner, E. Bauer, W. Steiner, and P. Rogl, Hyperfine Interact. **158**, 211 (2004).
[20] V. V. Krishnamurthy, J. C. Lang, D. Haskel, D. J. Keavney, G. Srajer, J. L. Robertson, B. C. Sales, D. G. Mandrus, D. J. Singh, and D. I. Bilc, Phys. Rev. Lett. **98**, 126403 (2007).
[21] B. T. Thole, P. Carra, F. Sette, and G. van der Laan, Phys. Rev. Lett. **68**, 1943 (1992); P. Carra, B. T. Thole, M. Altarelli, and Xindong Wang, *ibid.* **70**, 694 (1993).
[22] C. T. Chen, Y. U. Idzerda, H.-J. Lin, N. V. Smith, G. Meigs, E. Chaban, G. H. Ho, E. Pellegrin, and F. Sette, Phys. Rev. Lett. **75**, 152 (1995).

[23] G. van der Laan, B. T. Thole, G. A. Sawatzky, J. B. Goedkoop, J. C. Fuggle, J. M. Esteva, R. Karnatak, J. P. Remeika, and H. A. Dabkowska, Phys. Rev. B **34**, 6529 (1986).
[24] J. B. Kortright, D. D. Awschalom, J. Stöhr, S. D. Bader, Y. U. Idzerda, S. S. P. Parkin, I. K. Schuller, and H. C. Siegmann, J. Magn. Magn. Mater. **207**, 7 (1999).
[25] M. A. Laguna-Marco, J. Chaboy, and H. Maruyama, Phys. Rev. B **72**, 094408 (2005).
[26] C. Giorgetti, S. Pizzini, E. Dartyge, A. Fontaine, F. Baudelet, C. Brouder, Ph. Bauer, G. Krill, S. Miraglia, D. Fruchart, and J. P. Kappler, Phys. Rev. B **48**, 12732 (1993).
[27] M. S. S. Brooks, O. Eriksson, and B. Johansson, J. Phys.: Condens. Matter **1**, 5861 (1989).
[28] B. C. Sales, D. Mandrus, B. C. Chakoumakos, V. Keppens, and J. R. Thompson, Phys. Rev. B **56**, 15081 (1997).
[29] B. C. Sales, B. C. Chakoumakos, and D. Mandrus, Phys. Rev. B **61**, 2475 (2000).
[30] B. C. Sales, B. C. Chakoumakos, R. Jin, J. R. Thompson, and D. Mandrus, Phys. Rev. B **63**, 245113 (2001).
[31] B. C. Chakoumakos, B. C. Sales, and D. G. Mandrus, J. Alloys Compd. **322**, 127 (2001).
[32] S. Paschen, W. Carrillo-Cabrera, A. Bentien, V. H. Tran, M. Baenitz, Yu. Grin, and F. Steglich, Phys. Rev. B **64**, 214404 (2001).
[33] M. Suzuki, N. Kawamura, M. Mizumaki, A. Urata, H. Maruyama, S. Goto, and T. Ishikawa, Jpn. J. Appl. Phys., Part 2 **37**, L1488 (1998); J. Synchrotron Radiat. **6**, 190 (1999).
[34] G. Wortmann, I. Nowik, B. Perscheid, G. Kaindl, and I. Felner, Phys. Rev. B **43**, 5261 (1991).
[35] FEFF8 is an automated program for the multiple-scattering calculations of x-ray absorption fine structure and x-ray absorption near-edge structure for clusters of atoms. For further details, see http://leonardo.phys.washington.edu/feff/
[36] C. Godart, J. C. Achard, G. Krill, and M. F. Ravet-Krill, J. Less-Common Met. **94**, 177 (1983).
[37] B. T. Thole, G. van der Laan, J. C. Fuggle, G. A. Sawatzky, R. C. Karnatak, and J. M. Esteva, Phys. Rev. B **32**, 5107 (1985).
[38] M. Mizumaki, Y. Saitoh, A. Agui, K. Yoshii, A. Fujimori, and S. Nakamura, J. Synchrotron Radiat. **8**, 440 (2001).
[39] C. Kittel, *Introduction to Solid State Physics* (Wiley, New York, 1996).
[40] G. v. Gersdorff and C. Wetterich, Phys. Rev. B **64**, 054513 (2001); F. Jasch and H. Kleinert, J. Math. Phys. **42**, 52 (2001); M. Campostrini, M. Hasenbusch, A. Pelissetto, P. Rossi, and E. Vicari, Phys. Rev. B **65**, 144520 (2002).
[41] M. Campostrini, M. Hasenbusch, A. Pelissetto, P. Rossi, and E. Vicari, Phys. Rev. B **63**, 214503 (2001).
[42] S. Jia, S. L. Bud'ko, G. D. Samolyuk, and P. C. Canfield, Nat. Phys. **3**, 334 (2007).
[43] A. P. Holm, S. M. Kauzlarich, S. A. Morton, G. D. Waddill, W. E. Pickett, and J. G. Tobin, J. Am. Chem. Soc. **124**, 9894 (2002).
[44] D. M. Rowe, V. L. Kuznetsov, and L. A. Kuznetsova, in *Proceedings of the 17th International Conference on Thermoelectrics*, Nagoya, 24-28 May 1998, pp. 323–353.
[45] S. R. Brown, S. M. Kauzlarich, F. Gascoin, and G. J. Snyder, Chem. Mater. **18**, 1873 (2006).